Disruption of nontuberculous mycobacteria biofilms induces a highly vulnerable to antibiotic killing phenotype

Nikola Kurbatfinski [a], Preston J. Hill [c, 1], Noah Tobin [a], Cameron N. Kramer [a], Joseph Wickham [a], Steven D. Goodman [a, b], Luanne Hall-Stoodley [c], Lauren O. Bakaletz [a, b, *]

[a] *Center for Microbial Pathogenesis, Abigail Wexner Research Institute at Nationwide Children's Hospital, 700 Children's Drive, Columbus, OH, 43205, USA*
[b] *Department of Pediatrics, The Ohio State University College of Medicine, Columbus, OH, USA*
[c] *Department of Microbial Infection and Immunity, The Ohio State University, 460 W 12th Ave., Columbus, OH, 43210, USA*

ARTICLE INFO

ABSTRACT

Objectives: Structural or mucus hypersecretory pulmonary diseases such as cystic fibrosis (CF), wherein viscous mucus accumulates and clearance functions are impaired, predispose people to lung infection by inhaled bacteria that form biofilm aggregates. Nontuberculous mycobacteria (NTM), primarily *Mycobacterium abscessus* and *Mycobacterium avium,* are the growing cause of these lung infections and are extremely challenging to treat due to antibiotic recalcitrance. Better therapeutic approaches are urgently needed. We developed a humanized monoclonal antibody (HuTipMab) directed against a biofilm structural linchpin, the bacterial DNABII proteins, that rapidly disrupts biofilms and generates highly vulnerable newly released bacteria (NRel).
Methods: HuTipMab's ability to recognize HupB, NTM's DNABII homologue was determined by ELISA. Relative ability of HuTipMab to disrupt biofilms formed by lab-passaged and clinical isolates of NTM was assessed by CLSM. Relative sensitivity of NTM NRel to antibiotic killing compared to when grown planktonically was evaluated by plate count.
Results: HuTipMab recognized HupB and significantly disrupted NTM biofilms in a time- and dose-dependent manner. Importantly, NTM NRel of lab-passaged and clinical isolates were now highly sensitive to killing by amikacin and azithromycin.
Conclusions: If successful, this combinatorial treatment strategy would empower existing antibiotics to more effectively kill NTM newly released from a biofilm by HuTipMab and thereby both improve clinical outcomes and perhaps decrease length of antibiotic treatment for people that are NTM culture-positive.

1. Introduction

Nontuberculous mycobacteria (NTM), distantly related to *Mycobacterium tuberculosis*, cause chronic infections in people with structural or mucus hypersecretory pulmonary diseases, such as chronic obstructive pulmonary disease (COPD), primary ciliary dyskinesia (PCD), or CF [1, 2]. In lower airway biofilm infections such as in people with CF, PCD or COPD, mucociliary clearance is impeded by heavy sticky mucus and reduced airway surface liquid, by immotile or dysfunctional cilia and/or by damage to the respiratory epithelium [3]. Increased mucus

production by goblet cells is a common feature of CF, PCD and COPD [4]. These diseases were recently characterized as "muco-obstructive lung diseases" to better describe their clinical presentation of diffuse mucus obstruction, dilation of airway walls, prolonged inflammation and recurrent infection [5]. Muco-obstructive diseases in the lung therefore arise from different pathophysiological mechanisms that can involve defective epithelial cilia motility, ion transport and fluid homeostasis, or mucus secretion that results in the accumulation and stasis of mucus in airway compartments, which is not cleared and provides a microenvironment for persistent airflow obstruction, inflammation and

infection by growth of bacteria and development of biofilm aggregates [3].

NTM are classified as slow (e.g., *Mycobacterium avium, Mycobacterium kansasii, Mycobacterium marinum*) or rapidly growing [e.g., *Mycobacterium abscessus* complex (*Mycobacterium massiliense, Mycobacterium bollettii* and *Mycobacterium abscessus*), *Mycobacterium fortuitum, Mycobacterium chelonae*] [6], and in addition to genotypic/phenotypic variability, NTM prevalence varies with underlying lung diseases [7,8]. People with CF (PwCF) are highly vulnerable to lung infection and NTM are prevalent in both adults and children in the United States and Europe, with NTM prevalence increasing by 5% annually [1,9,10]. One in 5 PwCF are culture-positive for NTM [10] with acquisition associated with geographic region, increasing age, and NTM species.

Established NTM infections are extremely difficult to treat and require prolonged antibiotic therapy [1,2]. Recommended treatment for PwCF who are culture-positive for NTM is commonly a many years-long regimen of oral and intravenous antibiotics dependent on disease severity [1,2]. Despite these intense regimens, failure rate is high with up to 50%–60% of people unable to both transition from NTM-positive to NTM-negative sputum cultures and maintain this conversion for over 12 months particularly with *M. abscessus* [1,2]. Critically, 30%–60% of patients had to discontinue at least one of the prescribed antibiotics due to considerable treatment sequelae such as drug-related toxicity (e.g. nephrotoxicity or auditory-vestibular toxicity) [1]. In some cases, surgical resection may also be recommended or, dependent on severity, could be the only predictive curative therapy [2,8].

Reasons for treatment difficulty of NTM infections include low drug uptake due to thick, hydrophobic mycobacterial cell walls, export of drugs by efflux pumps, development of antibiotic resistance [7], and biofilm formation by NTM [11–15]. Biofilms are aggregated bacterial communities embedded in an extracellular polymeric substance (EPS) of proteins, carbohydrates and extracellular DNA (eDNA). They are phenotypically distinct from planktonic bacteria, and found in the lung and/or sputum of PwCF or COPD [3,13,16,17]. Biofilm-resident bacteria are well protected from antibiotics, chemical agents, mechanical stress and immune effectors through diverse mechanisms [18]. Further, they can tolerate antibiotics at many times the concentration required to kill their planktonic counterparts [11]. Canonically, clinical isolates are considered more virulent and more representative of disease-causative agents than their lab-passaged counterparts [19], as clinical isolates of *M. abscessus* display increased aggregation as well as intracellular survival and further, they induce greater inflammation relative to the reference strain, *M. abscessus* 19977 [20,21]. Thereby, consideration of testing clinical isolates in addition to lab-passaged strains is highly recommended [19].

Novel and more effective approaches to combat recalcitrant NTM infections are urgently needed [7]. We developed a targeted monoclonal antibody-based technology to disrupt biofilms and release resident bacteria into a transient phenotype that is more effectively killed by both antibiotics and human PMNs [22–25]. Interestingly, bacteria newly released from biofilm residence via a variety of mechanisms demonstrate this phenotype [26–29], however this unique phenotype is nonetheless not yet completely understood.

Our biofilm disruption strategy utilizes an antibody that targets an essential structural component of the biofilm [30,31], the bacterial DNA-binding proteins known as the DNABII family. When extracellular and within the biofilm matrix, DNABII proteins [HU (histone-like protein) and IHF (integration host factor)] serve as structural linchpins [16, 17,32] positioned at crossed strands of eDNA [32,33]. Anti-DNABII antibodies do not kill biofilm-resident bacteria [30,31], but instead induce an equilibrium shift of DNABII proteins away from their eDNA-bound state in the biofilm matrix to an unbound state in the extracellular milieu. Upon this equilibrium shift, the biofilm is rapidly disrupted to generate newly released (NRel) bacteria [24]. To date, using this targeted strategy, we've effectively disrupted biofilms formed by 23 bacterial genera *in vitro* [22,23,25,30,31,34], as well as *in vivo* using three distinct pre-clinical models of human disease [31,34,35].

Here, we investigated whether a humanized version of this DNABII-targeted monoclonal antibody (i.e., 'HuTipMab') could disrupt biofilms formed by both lab-passaged or clinical isolates of *M. abscessus* cultured from PwCF, as well as *M. avium*, to induce the formation of NTM NRel that were more susceptible to killing by two antibiotics commonly used to treat those with recalcitrant NTM infections.

2. Materials and methods

2.1. Antibodies

HuTipMab (in 100 mM HEPES, 100 mM NaCl, 50 mM NaOAc) is an IgG isotype and has been described [22]. Human IgG (HuIgG) [in phosphate buffered saline (PBS), without preservative] was used as the negative isotype control (Thermo Fisher Scientific, Inc., Waltham, MA).

2.2. Antibiotics

Amikacin sulfate salt and azithromycin dihydrate were purchased from Thermo Fisher Scientific, Inc. (Waltham, MA) and stored per manufacturer's instructions. Amikacin was suspended and diluted in Middlebrook 7H9 broth (BD Difco™, Franklin Lakes, NJ) with 0.2% glycerol and 10% albumin-dextrose-catalase (ADC, BD BBL™, Franklin Lakes, NJ) immediately prior to use. Azithromycin was suspended in dimethyl sulfoxide (Fisher Scientific International, Inc., Hampton, NH) then further diluted 1:1000 in 7H9 with 0.2% glycerol and 10% ADC immediately prior to use.

2.3. Bacterial strains and sources

M. abscessus 19977 (smooth morphotype) was originally isolated from an individual with a knee infection. *M. avium* 25291 was originally isolated from the infected liver of a chicken. Both isolates were procured from the American Type Culture Collection. *M. abscessus* clinical isolates 1, 2 and 3 (smooth morphotypes) were recovered from the sputum of PwCF. *M. abscessus* ATCC#19977 (Type strain *M. abscessus sensu stricto* subsp. *abscessus*) was used. This is the sequenced and established reference strain and contains both the smooth and rough morphotypes of *M. abscessus*. Clinical isolates of *M. abscessus* were also subspecies *abscessus* which has an active inducible erythromycin methylase (*erm41*) gene that typically impairs binding of macrolides to ribosomes to impart clinically significant macrolide resistance as well as other genetic features that are thought to contribute to antibiotic resistance [8,36]. *M. avium* ATCC#25291 (*M. avium* subsp. *avium)* was used. This serotype 2 strain is considered an environmental bacterium and opportunistic pathogen for humans, pigs and other species. This strain has been sequenced and is one of the most typically used strains to study antibiotic susceptibility and *M. avium* pathogenicity [37,38].

2.4. Isolation and purification of recombinant HupB

M. tuberculosis HupB was PCR amplified using the following oligonucleotides 5′–GCGTGCATATGAACAAAGCAGAGCTCATTGACGT–3′ and 5′–CGTGGCTCTTCCGCACGCTTTGCGACCCCGCCGAG–3′. Recombinant HupB was generated via previously described protocol [35], concentrated via centrifugal filter (3000 MWCO) and dialyzed against storage buffer (50 mmol Tris/L pH = 7.4, 600 mmol KCl/L, 1 mmol EDTA/L, 10% glycerol) then stored at −80 °C until used. Approximately 200 ng of recombinant HupB was separated by SDS-PAGE using a 4%–20% gradient gel at 5.6 V/cm for 1 h. Expected molecular mass of HupB = 28 kDa. Relative purity of HupB was determined by silver stain (Pierce™ Silver Stain Kit, Thermo Fisher Scientific, Inc., Waltham, MA).

2.5. Recognition of HupB by HuTipMab by ELISA

Purified recombinant HupB, tip-chimer peptide (a chimeric peptide which mimics protective epitopes of a DNABII protein and was used to generate HuTipMab, positive control), and tail-chimer peptide [35] (a chimeric peptide that mimics non-protective epitopes of a DNABII protein, negative control) were suspended in PBS (pH = 7.4). One μg of each was added to wells of a Falcon® 96-well plate in duplicate and incubated for 1 h at 37 °C. Fluid was removed and wells were washed twice with PBS containing 1:2000 v/v Tween™-20 (PBS-T). Wells were blocked with 3% dry milk in PBS-T for 1 h at 37 °C then washed twice with PBS-T. One set of the samples received 0.1 μg HuTipMab/well, whereas the other set received PBS-T alone (background control) after which all were incubated at 37 °C for 1 h. Wells were washed 3 times with PBS-T, followed by the addition of goat anti-human IgG conjugated to horseradish peroxidase (1:5000 dilution) (Novus Biologicals LLC, Centennial, CO) in PBS-T incubated at 37 °C for 1 h. Wells were washed 3 times with PBS-T and color was developed over 15 min at room temperature by addition of 1-Step™ Ultra TMB (Pierce™). Plates were read at 650 nm by FLUOstar Omega plate reader (BMG Labtech, Cary, NC) followed by visualization by Fluorchem M gel reader (ProteinSimple, Inc., Santa Clara, CA) with *trans*-UV light and 593 nm filter. Assays were repeated 3 times on separate days.

2.6. Biofilm formation by M. abscessus and M. avium

Stocks of *M. abscessus* or *M. avium* were maintained frozen in 7H9 broth containing 10% oleic acid-albumin-dextrose-catalase (OADC, Hardy Diagnostics, Santa Maria, CA), 30% glycerol and 0.05% Tween™-80 at 2×10^8 CFU/mL and stored at −80 °C. Stocks were gently thawed on ice, and bacteria pelleted by centrifugation at $21,100 \times g$ for 5 min at room temperature. Supernatants were discarded, pellet resuspended, and centrifuged again. Following centrifugation, bacteria were suspended to a final volume of 1 mL in 7H9 containing 10% OADC and 0.05% Tween™-80. Stocks were diluted ten-fold in 7H9/OADC/Tween™-80 to yield a final concentration of 2×10^7 CFU/mL, and 200 μL was used to inoculate each well of an 8-well chambered coverglass slide (Cellvis, Mountainview, CA). Biofilms of *M. abscessus* or *M. avium* were allowed to form at 37 °C and 5% CO_2 in a humidified atmosphere until the biofilms grew to a height of ∼30 μm as determined by confocal laser scanning microscopy (CLSM) and assessed by COMSTAT2. These incubation times were determined to be 72 h for *M. abscessus* versus 2 wks for slower growing *M. avium*. Biofilms of *M. abscessus* clinical isolates 1, 2 and 3 were also grown for an additional 24 h (96 h total) to evaluate whether HuTipMab could disrupt these even more mature biofilms.

2.7. Disruption of M. abscessus and M. avium biofilms by HuTipMab

Medium was aspirated from *M. abscessus* or *M. avium* biofilms, then they were gently washed twice with 200 μL equilibrated $1 \times$ Dulbecco's phosphate-buffered saline (DPBS) without calcium or magnesium (Corning, Corning, NY). Biofilms were then incubated with either 7H9 alone, 5 μg HuIgG, or with 5, 7.5 or 10 μg HuTipMab at 37 °C with 5% CO_2 in a humidified atmosphere for 30 min. To assay time-dependent disruption, additional wells were incubated with 5 μg HuTipMab for 60 min. After incubation, biofilms were gently washed once with 200 μL equilibrated DPBS. 7H9 medium was used as the diluent for all tested biologicals including the negative controls of human isotype IgG or medium-alone treated biofilms, against which all relative disruption comparisons were made. 7H9 medium used in all experiments contains 0.05% Tween™-80 and no other additives were added that disrupt biofilm growth. None of the components of the solvents in which HuIgG (PBS, no preservative) or HuTipMab (100 mM HEPES, 100 mM NaCl, 50 mM NaOAc) are dissolved contribute to biofilm disruption and both were further diluted in 7H9 medium prior to use.

Residual biofilm was stained with FM 1-43FX (Invitrogen) by incubation for 15 min statically in the dark. Stain was removed and biofilms were gently washed twice with DPBS then fixed for ≥3 h (1.6% paraformaldehyde, 2.5% glutaraldehyde and 4% acetic acid in 0.1 M phosphate buffer). Fixative was removed and replaced with DPBS then biofilms were visualized and imaged with a ZEISS CLSM800 microscope to select representative fields of view after review of the entire chamber within the chamberglass slide. Images were analyzed by COMSTAT2 to calculate relative biomass values ($\mu m^3/\mu m^2$). Values represent the mean of 3 biological replicates. Percent disruption was calculated as [mean biomass of wells treated with HuIgG - mean biomass of wells treated with HuTipMab]/[mean biomass of wells treated with HuIgG] x 100. Images selected are those that best represented the remaining biomass after disruption based upon review of the entire chamberslide. These images thereby align with the calculated average biomass value for each respective biofilm and treatment utilized.

2.8. Antibiotic mediated killing of newly released M. abscessus or M. avium

M. abscessus or *M. avium* biofilms were incubated with medium alone (for recovery of those bacteria growing/residing planktonically in the fluids above the biofilm) or 5 μg HuTipMab (to generate NRel) both with and without antibiotics. The concentration of each antibiotic that we used was a concentration that we pre-determined would limit killing of planktonic bacteria to ∼25%. This was done in order to facilitate our ability to detect any enhanced relative killing of NRel by the same concentration of antibiotic. For assay of relative killing of clinical *M. abscessus* isolates, we elected to test isolates 1 and 3 as these were more resistant to both amikacin and azithromycin (as reflected by their greater MIC values and concentrations needed to induce ∼25% killing) and thereby represented a more clinically relevant situation.

To determine relative susceptibility of planktonic NTM to amikacin, biofilms were prepared and gently washed twice with DPBS as described above, then treated with 200 μL of either: 7H9 (planktonic growth control); 7H9 + 0.5 μg amikacin/mL for *M. abscessus* 19977, + 12 μg amikacin/mL for *M. avium*, +0.7 μg amikacin/mL for *M. abscessus* clinical isolate 1 or +1 μg amikacin/mL for *M. abscessus* clinical isolate 3. To determine relative sensitivity of NTM NRel, biofilms were treated with 200 μL 7H9 + 5 μg HuTipMab alone (NRel growth control) or 7H9 + 5 μg HuTipMab + respective amikacin concentrations used above. Treated biofilms were incubated statically at 37 °C in 5% CO_2 and humidity for 2 h, after which 150 μL was collected from each well and dispensed into 1.5 mL Eppendorf microcentrifuge tubes, then pulse-vortexed with two sterile 3 mm glass beads (Fisher Scientific International, Inc., Hampton, NH) to disrupt aggregates. Suspensions were gently sonicated for 2 min in a waterbath sonicator (Ultrasonic Bath 2.8 L, Fisher Scientific) to further disrupt any aggregates. After sonication, samples were diluted and plated on Middlebrook 7H10 agar and incubated at 37 °C with 5% CO_2 in a humidified atmosphere to assess relative CFU.

To determine azithromycin-mediated killing, the same protocol as above was used with one adjustment. To avoid acidification of medium due to bacterial growth in wells to be treated with azithromycin which is unstable at lower pH [39], these cultures were incubated for 2 h at 37 °C without 5% CO_2. Wells were treated with 200 μL of either: 7H9 (growth control); 7H9 + 5 μg azithromycin/mL for *M. abscessus* 19977, +16 μg azithromycin/mL for *M. avium*, +10 μg azithromycin/mL for *M. abscessus* clinical isolate 1, or +8 μg azithromycin/mL for *M. abscessus* clinical isolate 3. To determine relative sensitivity of NTM NRel, biofilms were treated with 200 μL 7H9 + 5 μg HuTipMab (NRel growth control) or 7H9 + 5 μg HuTipMab + respective azithromycin concentrations used above. Percent killing was then calculated as [growth control CFU/mL - NRel or planktonic CFU/mL]/[growth control CFU/mL] x 100. All assays were repeated a minimum of 3 times on separate days with 2 technical replicates conducted on each of those separate days.

2.9. Statistical analysis

Results are expressed as mean ± SD of 3 biological replicates with 2–3 technical replicates each. Comparisons between groups were made with unpaired t-tests. All statistical analyses were performed with Graphpad (Prism) software V9.

3. Results

3.1. Validation of HuTipMab specificity

Purity of isolated recombinant HupB was confirmed via silver stain (Fig. 1A). Recognition of HupB by HuTipMab was shown via ELISA wherein HuTipMab recognized both HupB and the tip-chimer peptide (positive control peptide against which HuTipMab was derived); no color developed in the absence of HuTipMab ($P < 0.001$–0.0001) (Fig. 1B and C). HuTipMab did not recognize the tail-chimer peptide as expected as this peptide is a negative control for immune recognition by this monoclonal antibody.

3.2. Assessment of relative HuTipMab-induced NTM biofilm disruption by CLSM

We next determined HuTipMab's biofilm disruption capabilities by

incubation of 72 h *M. abscessus* 19977 biofilms or 2 wk *M. avium* biofilms with increasing concentrations of, or an increased incubation period with, HuTipMab. After incubation, NRel were removed and the residual biofilms visualized by CLSM. COMSTAT2 image analysis revealed that HuTipMab disrupted *M. abscessus* 19977 biofilms significantly more than biofilms incubated with medium alone or with HuIgG ($P < 0.01$–0.0001) (Fig. 2A and B). Additionally, *M. abscessus* 19977 biofilms were disrupted in a dose- and time-dependent manner as a 30 min incubation with 5, 7.5 or 10 µg HuTipMab resulted in 53%, 79% or 88% disruption respectively, whereas disruption was 89% when incubated with 5 µg HuTipMab for 60 min.

We also similarly conducted a preliminary evaluation of our ability to disrupt a biofilm formed by a single isolate of *M. avium* and found that these biofilms were also significantly disrupted by incubation with HuTipMab ($P < 0.01$–0.0001) (Fig. 3A and B). This disruption was again dose- and time-dependent wherein disruption by HuTipMab at 5, 7.5 or 10 µg for 30 min was 51%, 68% or 76%, respectively whereas when incubated with 5 µg HuTipMab for 60 min, disruption was 80%.

Significant dose- and time-dependent disruption of 72 h biofilms formed by all 3 clinical isolates of *M. abscessus* was also evident ($P < 0.001$–0.0001) (Fig. 4A–F). Disruption by HuTipMab at 5, 7.5 or 10 µg for 30 min was 57%–62%, 77%–88% or 89%–93%, respectively whereas when incubated with 5 µg HuTipMab for 60 min, disruption was 90%–92%. The more mature 96 h biofilms formed by these 3 clinical isolates
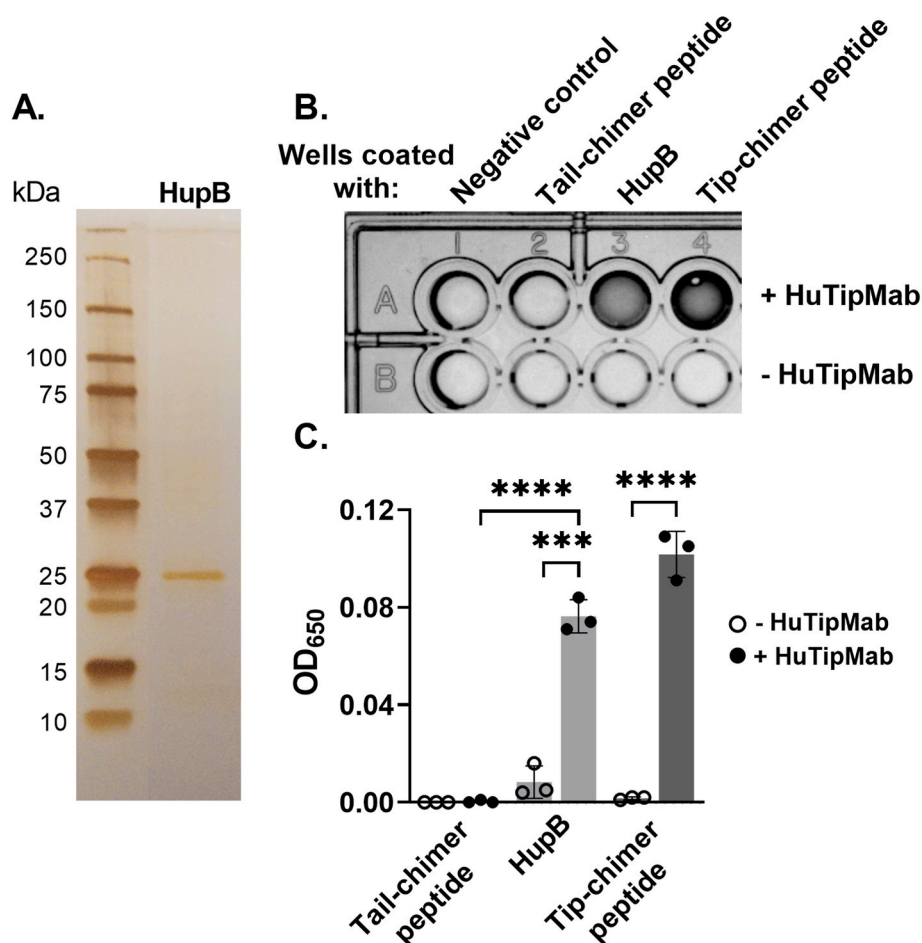
Fig. 1. HuTipMab recognized the isolated NTM DNA-binding protein HupB. *Panel A*: Silver-stained gel of SDS-PAGE-separated protein revealed pure protein isolation with band at anticipated location based on the following expected molecular mass of protein monomer: HupB = 28 kDa. *Panel B*: Specificity of HuTipMab to tail-chimer peptide (negative control; immunogen against which antibodies have no therapeutic or protective effect) [35], HupB, and tip-chimer peptide (positive control; antigenic target of HuTipMab and against which antibodies have significant therapeutic protective effect) was determined via ELISA. Dark wells of representative image of ELISA plate indicated reactivity of HuTipMab to HupB and tip-chimer peptide. *Panel C*: Color developed in wells of ELISA plates was quantified via plate reader by measurement of optical density at 650 nm. Reactivity of HuTipMab to HupB and tip-chimer peptide was significantly greater than that to tail-chimer peptide, which showed no reactivity. Statistically significant differences in optical density are reported as ***, $P \leq 0.001$; ****, $P < 0.0001$.

A.

B.
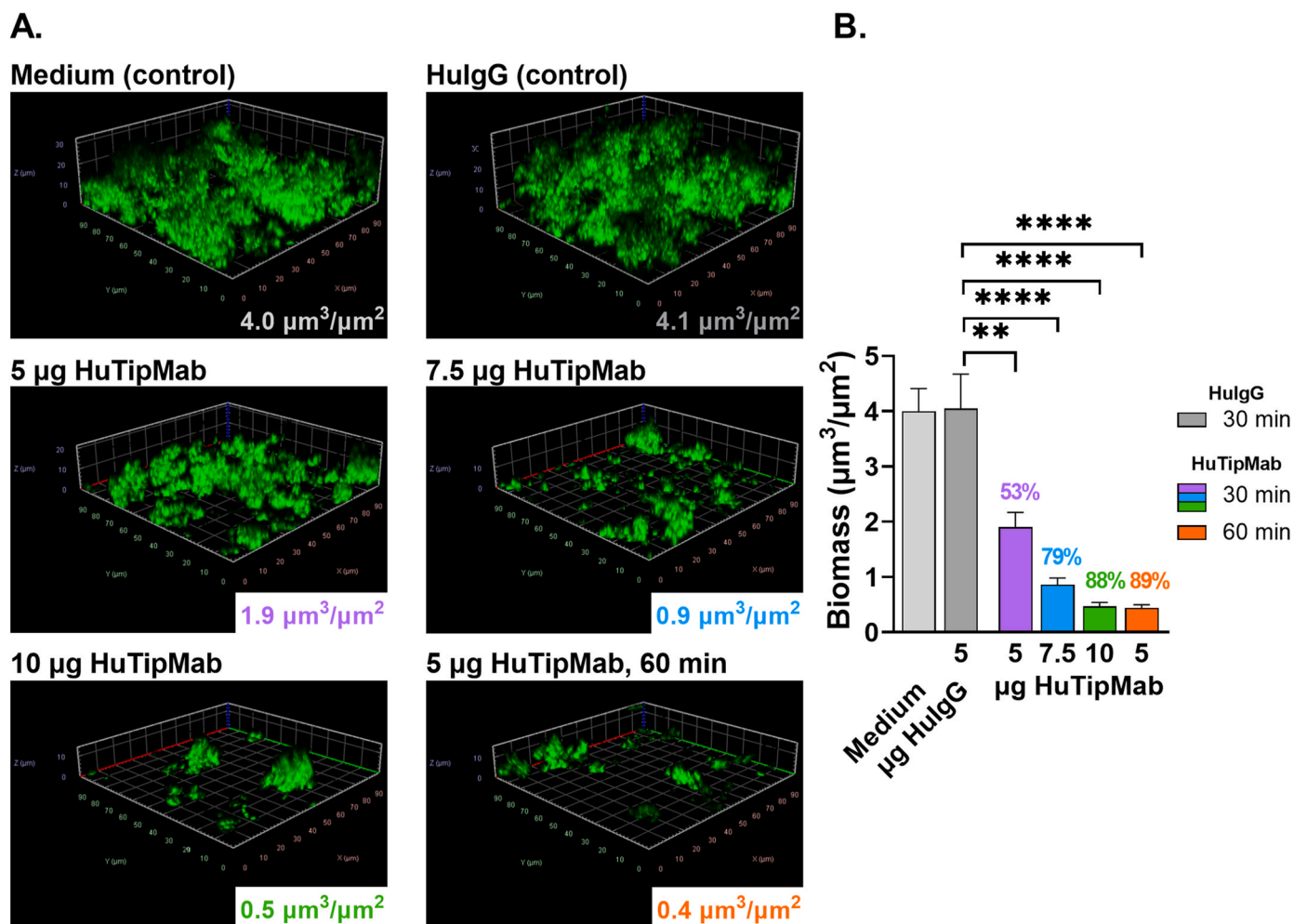
Fig. 2. HuTipMab disrupted 72 h M. *abscessus* 19977 biofilms in a dose- and time-dependent manner. *Panel A*: Representative 3-dimensional images of *M. abscessus* 19977 biofilms incubated with medium alone, 5 μg HuIgG, or 5, 7.5, or 10 μg HuTipMab, stained with FM 1-43FX (green), fixed and visualized by CLSM. Biomass was calculated via COMSTAT2 and mean biomass values post-incubation for each treatment are in lower right portion of each image. All treatments were incubated for 30 min unless noted otherwise (bottom right image from biofilms treated with 5 μg HuTipMab for 60 min). *M. abscessus* 19977 biofilms treated with HuTipMab displayed a marked relative reduction in biomass and height as compared to biofilms incubated with medium or HuIgG. *Panel B:* Graphed mean biomass values of each treatment. There was no significant difference in biomass between wells incubated with medium alone or 5 μg HuIgG. Relative to HuIgG incubation, all wells incubated with HuTipMab were significantly reduced in biomass from 53% to 89% biofilm disruption. Statistically significant differences in biomass are reported as **, P ≤ 0.01; ****, P < 0.0001. Images selected are those that best represent the calculated average biomass value for said biofilm and treatment.

were similarly significantly disrupted by HuTipMab with relative mean percent disruption of 57%–59%, 76%–89% or 89%–94% when incubated with 5, 7.5 or 10 μg for 30 min, respectively and 90%–93% when incubated with 5 μg HuTipMab for 60 min (P < 0.05–0.0001) (data not shown).

3.3. Enhanced killing of NTM NRel by antibiotics commonly used to treat NTM infections

To determine whether NTM NRel demonstrated heightened antibiotic susceptibility, we assessed relative killing by amikacin and azithromycin. Killing of planktonic *M. abscessus* 19977 by amikacin or azithromycin was limited to 23% and 20%, respectively whereas *M. abscessus* 19977 NRel were significantly more sensitive to both antibiotics with killing at 61% and 42%, respectively (Fig. 5A and B) (P < 0.001 or 0.01, respectively). Notably, this enhanced killing occurred when amikacin and azithromycin were used at 1/4 and 1/2 the reported minimum inhibitory concentrations (MIC), respectively.

Similarly, *M. avium* NRel were significantly more susceptible to antibiotic killing than their isogenic planktonic counterparts with percent killing of planktonic *M. avium* limited to 17% and 19% by

amikacin and azithromycin, respectively, whereas that for *M. avium* NRel was 41% and 36%, respectively (P < 0.01) (Fig. 6A and B). This significantly enhanced susceptibility of *M. avium* NRel to killing by amikacin and azithromycin was observed when used at 1/4 and 1/2 the respective MICs.

NRel from disrupted 72 h biofilms formed by *M. abscessus* clinical isolates 1 or 3 were also significantly more susceptible to killing by amikacin and azithromycin than their isogenic planktonic counterparts (P < 0.05–0.001) (Fig. 7A–D). Percent killing of planktonic *M. abscessus* was limited to 28% and 28% for clinical isolate 1 and 21% and 25% for clinical isolate 3 by amikacin and azithromycin, respectively, whereas killing of NRel was 45% and 47% for clinical isolate 1 or 47% and 45% by amikacin and azithromycin, respectively for clinical isolate 3. The significantly greater percent killing of NRel compared to that of their planktonic population was achieved with 1/6 and 1/3 of the MIC of amikacin and azithromycin, respectively for clinical isolate 1 or with 1/4 and 1/4 of the MIC of amikacin and azithromycin, respectively for clinical isolate 3.

A.

B.
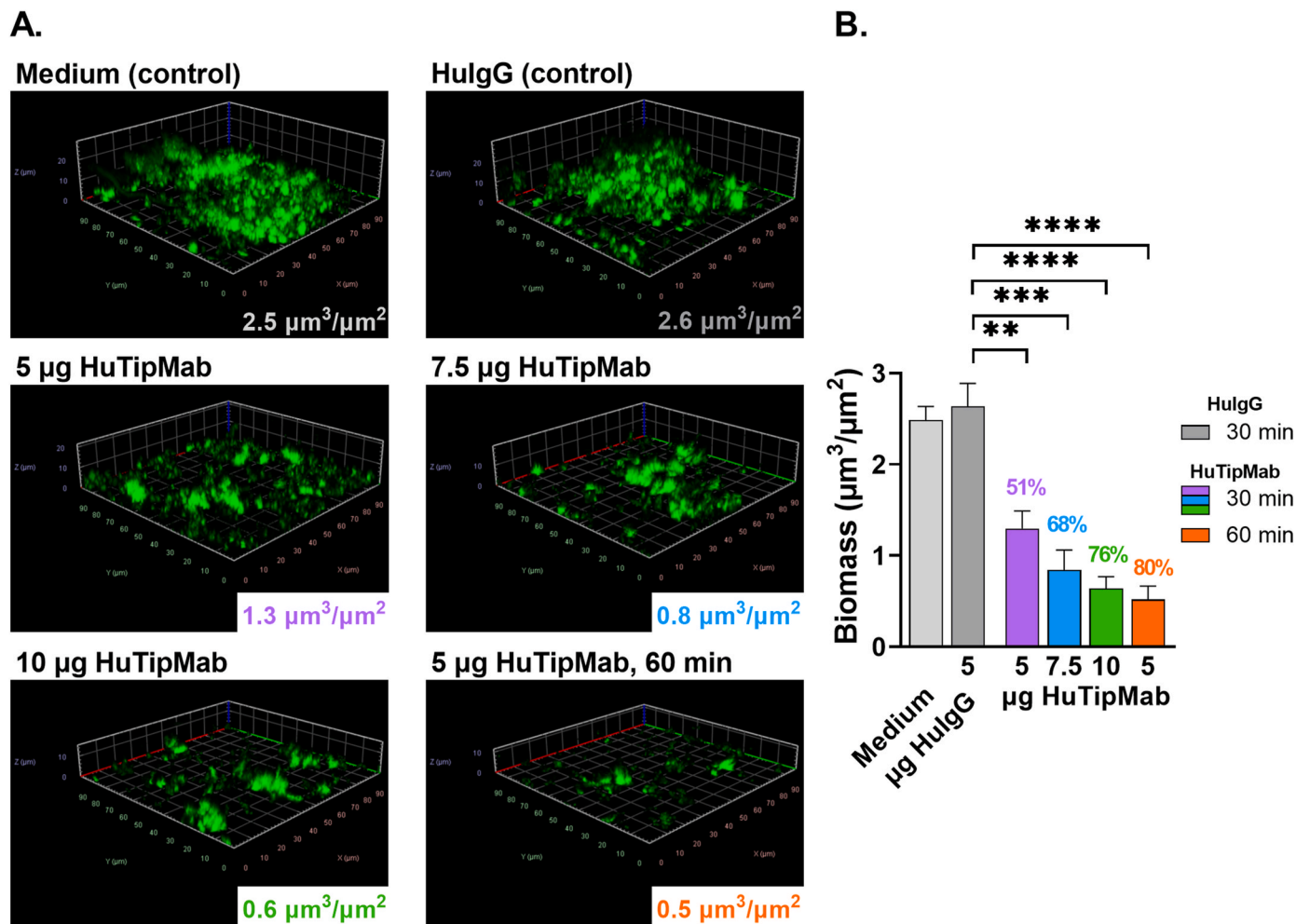
Fig. 3. HuTipMab-induced disruption of 2 wk M. *avium* biofilms was dose- and time-dependent. *Panel A:* Post-incubation of *M. avium* biofilms with medium alone, 5 μg HuIgG, or 5, 7.5, or 10 μg HuTipMab for 30 min unless noted otherwise (bottom right image from biofilms treated with 5 μg HuTipMab for 60 min), biofilms were stained with FM 1-43FX (green), fixed and visualized via CLSM. Biomass was calculated via COMSTAT2 and mean biomass values post-incubation for each treatment are in lower right portion of each image. Biomass and height of *M. avium* biofilms incubated with HuTipMab were notably reduced compared to that seen in wells incubated with medium alone or 5 μg HuIgG. *Panel B*: Mean biomass values of biofilms incubated with each treatment condition represented graphically. Biomass values from wells incubated with medium alone or 5 μg HuIgG were not significantly different. However, when biofilms were incubated with HuTipMab, biomass values were significantly reduced as compared to those incubated with HuIgG alone with percent biomass disruption ranging from 51% to 80%. Statistically significant differences in biomass are reported as **, P ≤ 0.01; ***, P ≤ 0.001; ****, P < 0.0001. Images selected are those that best represent the calculated average biomass value for said biofilm and treatment.

4. Discussion

Antibiotic therapy for PwCF who are culture-positive for NTM involves a prolonged regimen with multiple antibiotics, the potential for multiple sequelae, and an unacceptably high rate of clinical failure which could further necessitate lung resection for disease resolution in other lung diseases such as COPD [1,2,8]. While modulator therapy both reduces symptoms and frequency of NTM-positive cultures, it remains to be determined if this latter outcome is due to reduced ability to collect sputum, or a true decline in NTM prevalence [40]. Additionally, modulator treatment remains inaccessible to a majority of PwCF due to both cost and availability that is currently limited to the US, Europe, Australia, and New Zealand [41]. New strategies to enhance the effectiveness of existing antibiotic therapies are thus warranted, particularly given that there is now rather limited investment in new antibiotic discovery [42]. Novel approaches including those that target the biofilm matrix to release resident bacteria for elimination by either antibiotics or host immune effectors are a high priority [7,18].

We developed such a strategy using an epitope-targeted monoclonal antibody against the DNABII proteins. This approach effectively disrupts

biofilms formed *in vitro* by 23 bacterial genera [22,23,30,31,34], as well as biofilms formed *in vivo* in three distinct pre-clinical disease models [31,34,35]. Further, we have shown that bacteria newly released from biofilms formed by ten diverse pathogens are significantly more sensitive to antibiotic-mediated killing. Typically NRel are even more sensitive than when planktonically grown, the latter of which had heretofore been considered the most vulnerable to antibiotic-mediated killing [22, 23]. While this approach appears to be species agnostic for all tested pathogens to date, the majority of those tested were Gammaproteobacteria. We therefore now wanted to determine if HuTipMab treatment would also be effective against NTM, which belong to the class Actinomycetia and are distinguished by a thick, mycolic acid-rich cell wall.

Comparative genomics showed that NTM can express a DNABII homologue and *in silico* analysis revealed that mycobacterial HUs have two domains. The N-terminal 106 amino acid (AA) domain has high similarity to other DNABII proteins (all are ~90–105 AAs in length), whereas the 108 amino acid C-terminal domain has a eukaryotic H1 histone-like motif. Further, 104 out of 106 AAs within the translated sequence of the N-terminal DNABII-like domain are identical between the HU proteins expressed by *M. tuberculosis* and *M. avium,* whereas 99 out of 106 perfect
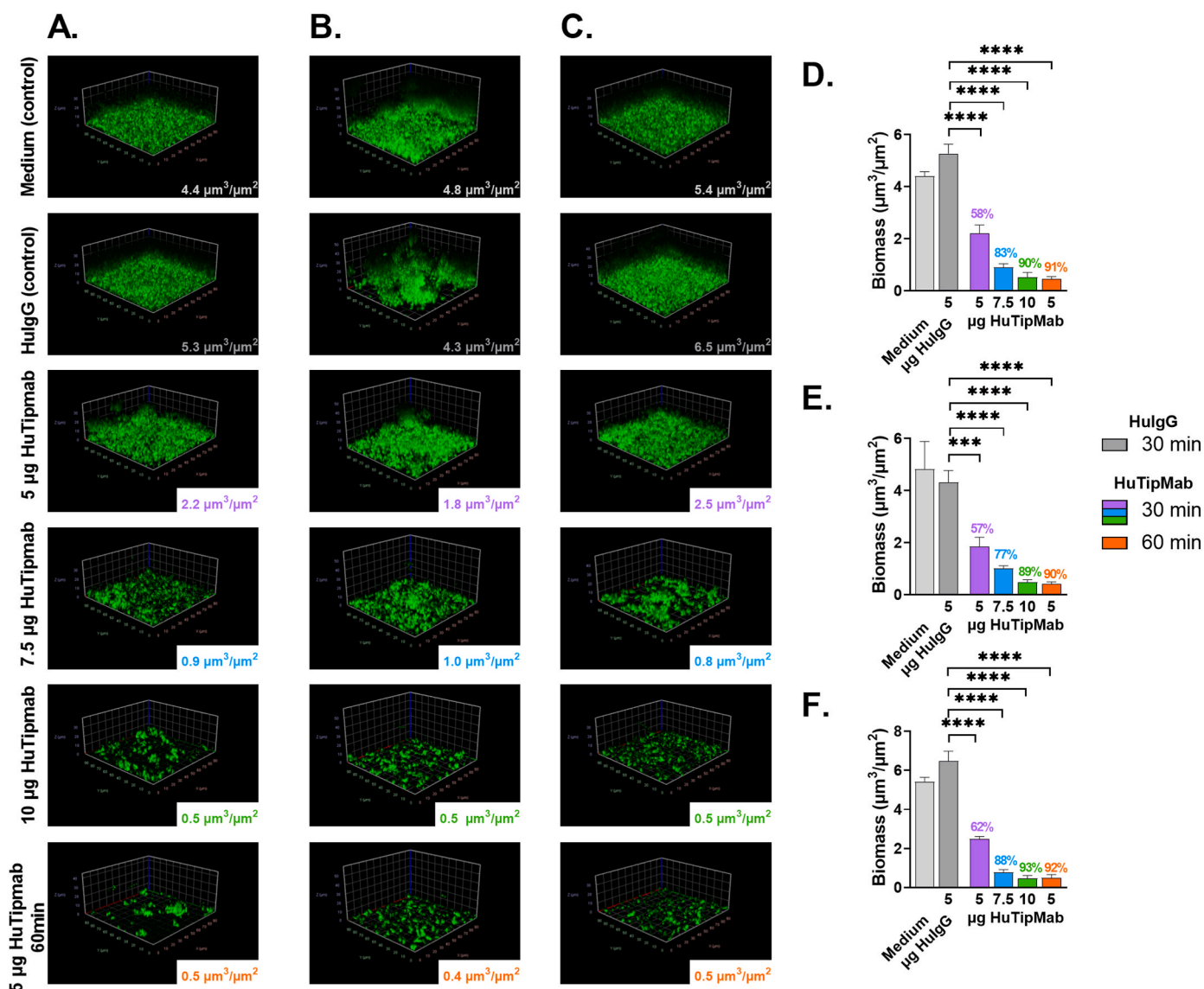
Fig. 4. Disruption of 72 h biofilms formed by 3 isolates of *M. abscessus* cultured from PwCF by HuTipMab was also dose- and time-dependent. *Panels A, B & C*: Representative 3D images of biofilms of *M. abscessus* clinical isolates 1, 2 and 3 respectively post-incubation with medium alone, 5 µg HuIgG, or 5, 7.5, or 10 µg HuTipMab for 30 min unless noted otherwise (bottom images were captured from biofilms treated for 60 min with 5 µg HuTipMab). Biofilms were stained with FM 1-43FX (green), fixed and visualized via CLSM. Biomass was calculated via COMSTAT2 and mean biomass values post-incubation for each treatment are in lower right portion of each image. Incubation with HuTipMab notably reduced biomass and height of biofilms compared to incubation with medium alone or 5 µg HuIgG. *Panel D, E & F*: Graphical representation of mean biomass values for biofilms formed by *M. abscessus* clinical isolates 1, 2 and 3 respectively post-incubation with each treatment condition. Disruption was significant for each HuTipMab treatment relative to treatment with HuIgG, which was never significantly different from wells treated with medium alone. Percent biomass disruption for clinical isolate 1 ranged from 58% to 91%, for clinical isolate 2 ranged from 57% to 90%, and for clinical isolate 3 ranged from 62% to 93%. Statistically significant differences in biomass are reported as ***, P ≤ 0.001; ****, P < 0.0001. Images selected are those that best represent the calculated average biomass value for said biofilm and treatment.

matches for HU expressed by *M. abscessus.* All three DNABII homologues expressed by these mycobacterial species share at least 37 consecutive identical AAs, which comprise the tip region against which HuTipMab is targeted and which likely accounts for its ability to recognize HupB of *M. tuberculosis* by ELISA. Both *M. abscessus* and *M. avium* form biofilms that incorporate eDNA into the EPS matrix [12,14,15], however it was unknown whether these biofilms also incorporated DNABII proteins within the eDNA-rich biofilm matrix nor was it known whether HuTipMab, generated against specific protective domains of a traditional DNABII protein would both recognize the unique mycobacterial DNABII homologue and actively disrupt NTM biofilms. We show here that HuTipMab did indeed effectively disrupt biofilms formed by both *M. abscessus* and *M. avium* in a dose- and time-dependent manner which indicated that HuTipMab retained recognition and biofilm-disruptive

capabilities against NTM, inclusive of biofilms formed by *M. abscessus* isolates recovered from PwCF, which likely better represent *M. abscessus* found in the disease site.

Once disrupted, NRel of *M. abscessus* 19977, *M. abscessus* clinical isolates 1 and 3, as well as NRel of *M. avium*, displayed increased susceptibility to two clinically relevant antibiotics. NTM NRel were significantly more sensitive to amikacin and azithromycin compared with their isogenic planktonic counterparts, two antibiotics which are ineffective when NTM reside within a biofilm [11]. Notably, enhanced antibiotic susceptibility of NRel occurred at fractions of the planktonic MIC for *M. abscessus* and *M. avium*. This outcome is likely to have been aided by the fact that amikacin and azithromycin have greater access to their targets after release of NTM from their protective biofilms.

Given that biomass disruption ranged from 51% to 92% across all
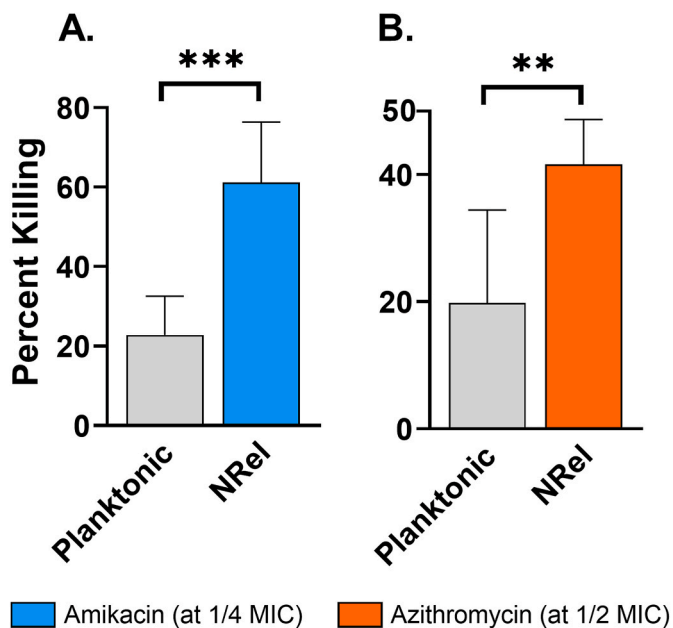
Fig. 5. *M. abscessus* 19977 NRel were significantly more susceptible to amikacin and azithromycin. As compared to killing of planktonic, killing of NRel was significantly greater for both amikacin and azithromycin, notably at 1/4 and 1/2 the MIC. Killing of planktonic was 23% and 20% respectively and killing of NRel was 61% and 42% respectively. Statistically significant differences in percent killing are reported as **, $P \leq 0.01$; ***, $P \leq 0.001$.
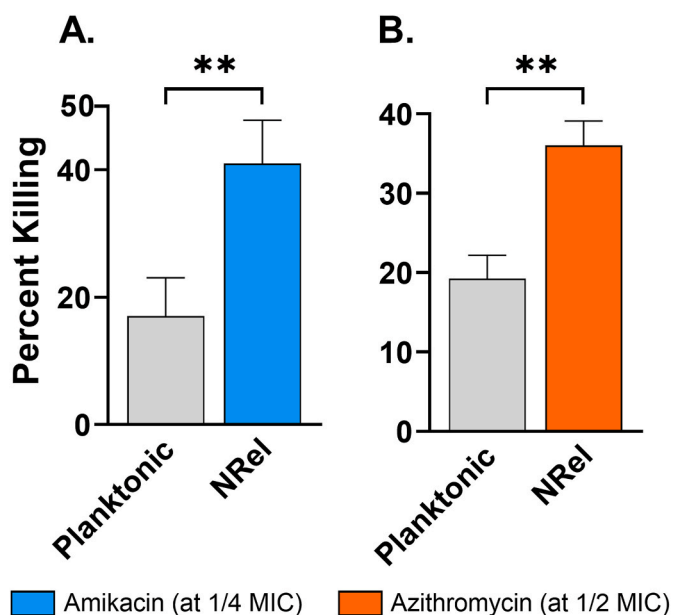
Fig. 6. HuTipMab-induced *M. avium* NRel were significantly sensitized to amikacin and azithromycin. When tested against both amikacin and azithromycin, 2 antibiotics used to treat NTM in PwCF, NRel were significantly more sensitive to antibiotic killing than planktonic *M. avium*. In combination with amikacin at 1/4 MIC, killing of planktonic *M. avium* was 17% while killing of *M. avium* NRel was 41%. Similarly, incubation of planktonic *M. avium* with 1/2 MIC of azithromycin resulted in 19% killing while incubation of *M. avium* NRel at the same concentration resulted in 36% killing. Statistically significant differences in percent killing are reported as **, $P \leq 0.01$.

biofilms tested in this study, the possibility remains that any remaining bacteria could grow to reestablish a biofilm and maintain infection. However, the demonstrated dose- and time-dependence of HuTipMab-

induced disruption suggests that modulation of the dose and/or treatment duration could reduce the biofilm to a monolayer of cells that could then be cleared by antibiotics and/or immune effectors as we have shown in 3 distinct preclinical models of disease to date [30,31,34,35]. In each of these studies there was both rapid clearance of bacteria and disease resolution. In one study, to directly test whether any residual biomass would regrow and re-initiate infection, we continued to monitor disease status for 1 week after cessation of treatment with no evidence of reinfection observed [43]. Additionally, we recently showed that bacteria within any limited biomass that remains after HuTipMab-mediated disruption and removal of NRel are also significantly more sensitive to the killing action of antibiotics than that of an undisrupted biofilm [23]. Nonetheless, we are currently expanding upon these *in vitro* studies into those performed with polarized human airway epithelial cell cultures as well as a murine model of *M. abscessus*-induced lung infection. Additionally, we hope to determine if the phenotype of enhanced sensitivity to antibiotics extends to clinical isolates of *M. avium* recovered from the lungs of PwCF, as well as whether the demonstrated sensitivity extends to other antibiotics used to treat NTM for those who may not be able to tolerate either amikacin or azithromycin.

New data presented here provide strong support for a combinatorial therapeutic strategy for those infected with NTM, where biofilms contribute significantly to decline in lung function and poor quality of life [2,13]. We envision nebulizing HuTipMab, as has been successfully done with IgG [44], into the lungs of these individuals or delivering HuTipMab intravenously, as is currently being tested in a clinical trial of community-acquired pneumonia (NCT05629741), to disrupt biofilm aggregates and release NTM from the antibiotic-tolerant biofilm into the NRel state such that co-delivered antibiotics could rapidly kill the induced NTM NRel. If successful, this strategy would empower existing antibiotics, improve clinical outcomes and perhaps also decrease the length of antibiotic treatment for PwCF, as well as the growing population of people with other pulmonary diseases or without any other underlying disease, but who nonetheless have a recalcitrant NTM infection [1,2,45].

Funding statement

Ethical approval

The current work does not involve experimental work with humans or animals.

Declaration of interests

The authors declare the following financial interests/personal relationships which may be considered as potential competing interests:

Lauren O. Bakaletz reports financial support was provided by Cystic Fibrosis Foundation. Steven D Goodman reports financial support was provided by Cystic Fibrosis Foundation. Luanne Hall-Stoodley reports financial support was provided by Cystic Fibrosis Foundation. L.O.B. and S.D.G. are inventors of technology related to the DNABII-directed approach, rights to which have been licensed to Clarametyx Biosciences, Inc.

CRediT authorship contribution statement

Nikola Kurbatfinski: Methodology, Validation, Formal analysis,
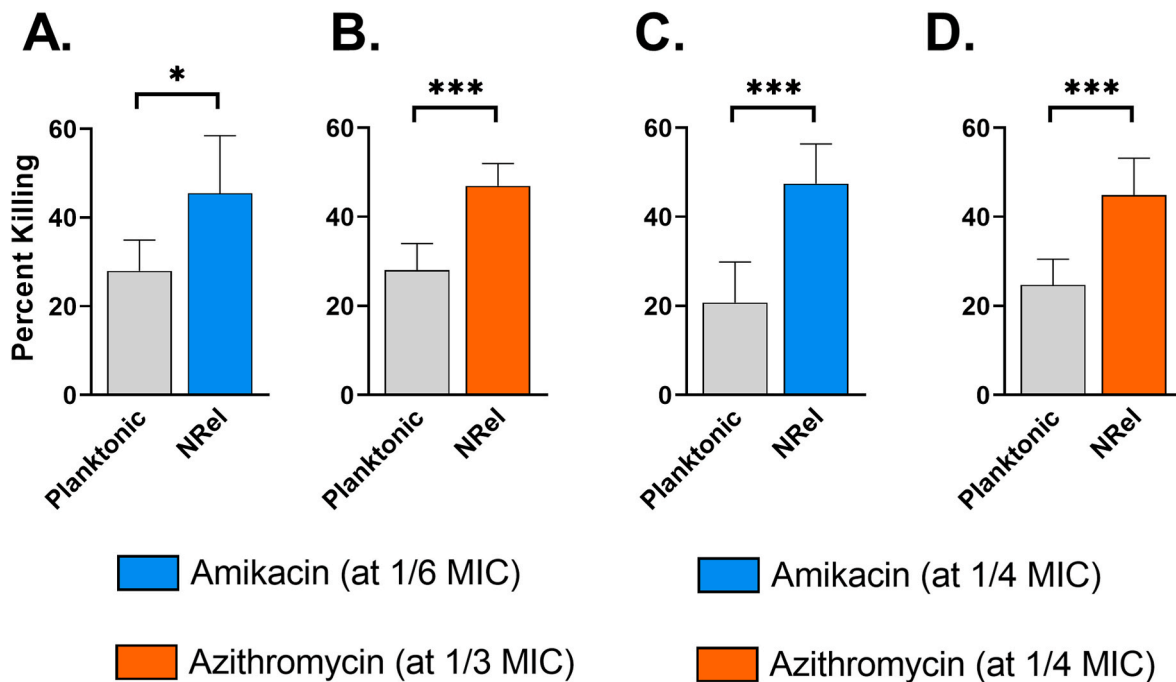
Fig. 7. HuTipMab-induced NRel of *M. abscessus* clinical isolates 1 and 3 were significantly sensitized to killing by amikacin and azithromycin than when grown planktonically. *Panels A & B:* In combination with 1/6 the planktonically determined MIC of amikacin, killing of planktonic *M. abscessus* clinical isolate 1 was 28% whereas that of this clinical isolate's HuTipMab-induced NRel was 45%. Similarly, incubation of planktonic *M. abscessus* clinical isolate 1 with 1/3 the planktonically determined MIC of azithromycin resulted in 28% killing whereas killing of *M. abscessus* clinical isolate 1 NRel at the same concentration was 47%. *Panels C & D:* Killing of planktonic *M. abscessus* clinical isolate 3 by amikacin was 21% whereas killing of the corresponding NRel was 47%. Similarly, azithromycin killed 45% of *M. abscessus* clinical isolate 3 NRel at the same concentration that killed 25% of planktonic *M. abscessus* clinical isolate 3. Notably, this significant increase in antibiotic killing of *M. abscessus* clinical isolate 3 was observed at 1/4 the MIC for each antibiotic. Statistically significant differences in percent killing are reported as *, P ≤ 0.05; ***, P ≤ 0.001.

Investigation, Writing – original draft, Writing – review & editing, Visualization, Project administration. **Preston J. Hill:** Methodology, Validation, Resources, Writing – review & editing. **Noah Tobin:** Methodology, Validation, Formal analysis, Investigation, Visualization. **Cameron N. Kramer:** Validation, Formal analysis, Investigation, Visualization. **Joseph Wickham:** Methodology, Validation, Formal analysis, Investigation, Resources, Visualization. **Steven D. Goodman:** Conceptualization, Methodology, Writing – review & editing, Funding acquisition. **Luanne Hall-Stoodley:** Conceptualization, Methodology, Writing – review & editing, Funding acquisition, Supervision. **Lauren O. Bakaletz:** Conceptualization, Methodology, Writing – review & editing, Funding acquisition, Supervision, Project administration.

Data availability

Data will be made available on request.

References

[1] Floto RA, Olivier KN, Saiman L, Daley CL, Herrmann JL, Nick JA, et al. US Cystic Fibrosis Foundation and European Cystic Fibrosis Society consensus recommendations for the management of non-tuberculous mycobacteria in individuals with cystic fibrosis. Thorax 2016;71(Suppl 1):i1–22. https://doi.org/10.1136/thoraxjnl-2015-207360.
[2] Griffith DE, Aksamit T, Brown-Elliott BA, Catanzaro A, Daley C, Gordin F, et al. An official ATS/IDSA statement: diagnosis, treatment, and prevention of nontuberculous mycobacterial diseases. Am J Respir Crit Care Med 2007;175:367–416. https://doi.org/10.1164/rccm.200604-571ST.
[3] Hall-Stoodley L, McCoy KS. Biofilm aggregates and the host airway-microbial interface. Front Cell Infect Microbiol 2022;12:969326. https://doi.org/10.3389/fcimb.2022.969326.
[4] Davis JD, Wypych TP. Cellular and functional heterogeneity of the airway epithelium. Mucosal Immunol 2021;14:978–90. https://doi.org/10.1038/s41385-020-00370-7.
[5] Boucher RC. Muco-obstructive lung diseases. N Engl J Med 2019;380:1941–53. https://doi.org/10.1056/NEJMra1813799.
[6] Tortoli E, Kohl TA, Brown-Elliott BA, Trovato A, Leao SC, Garcia MJ, Vasireddy S, Turenne CY, Griffith DE, Philley JV, Baldan R, Campana S, Cariani L, Colombo C, Taccetti G, Teri A, Niemann S, Wallace Jr RJ, Cirillo DM. Emended description of *Mycobacterium abscessus, Mycobacterium abscessus* subsp. *abscessus* and *Mycobacterium abscessus* subsp. *bolletii* and designation of *Mycobacterium abscessus* subsp. *massiliense* comb. nov. Int J Syst Evol Microbiol 2016;66:4471–9. https://doi.org/10.1099/ijsem.0.001376.
[7] Daniel-Wayman S, Abate G, Barber DL, Bermudez LE, Coler RN, Cynamon MH, Daley CL, Davidson RM, Dick T, Floto RA, Henkle E, Holland SM, Jackson M, Lee RE, Nuermberger EL, Olivier KN, Ordway DJ, Prevots DR, Sacchettini JC, Salfinger M, Sassetti CM, Sizemore CF, Winthrop KL, Zelazny AM. Advancing translational science for pulmonary nontuberculous mycobacterial infections. A road map for research. Am J Respir Crit Care Med 2019;199:947–51. https://doi.org/10.1164/rccm.201807-1273PP.
[8] Swenson C, Zerbe CS, Fennelly K. Host variability in NTM disease: implications for research needs. Front Microbiol 2018;9:2901. https://doi.org/10.3389/fmicb.2018.02901.
[9] Dahl VN, Molhave M, Floe A, van Ingen J, Schon T, Lillebaek T, Andersen AB, Wejse C. Global trends of pulmonary infections with nontuberculous mycobacteria: a systematic review. Int J Infect Dis 2022;125:120–31. https://doi.org/10.1016/j.ijid.2022.10.013.
[10] Prieto MD, Alam ME, Franciosi AN, Quon BS. Global burden of nontuberculous mycobacteria in the cystic fibrosis population: a systematic review and meta-analysis. ERJ Open Res 2023;9. https://doi.org/10.1183/23120541.00336-2022.
[11] Clary G, Sasindran SJ, Nesbitt N, Mason L, Cole S, Azad A, McCoy K, Schlesinger LS, Hall-Stoodley L. *Mycobacterium abscessus* smooth and rough morphotypes form antimicrobial-tolerant biofilm phenotypes but are killed by acetic acid. Antimicrob Agents Chemother 2018;62. https://doi.org/10.1128/AAC.01782-17.
[12] Munoz-Egea MC, Akir A, Esteban J. *Mycobacterium* biofilms. Biofilms 2023;5:100107. https://doi.org/10.1016/j.bioflm.2023.100107.

[13] Qvist T, Eickhardt S, Kragh KN, Andersen CB, Iversen M, Hoiby N, Bjarnsholt T. Chronic pulmonary disease with *Mycobacterium abscessus* complex is a biofilm infection. Eur Respir J 2015;46:1823–6. https://doi.org/10.1183/13993003.01102-2015.

[14] Rose SJ, Babrak LM, Bermudez LE. *Mycobacterium avium* possesses extracellular DNA that contributes to biofilm formation, structural integrity, and tolerance to antibiotics. PLoS One 2015;10:e0128772. https://doi.org/10.1371/journal.pone.0128772.

[15] Rose SJ, Bermudez LE. Identification of bicarbonate as a trigger and genes involved with extracellular DNA export in mycobacterial biofilms. mBio 2016;7. https://doi.org/10.1128/mBio.01597-16.

[16] Gunn JS, Bakaletz LO, Wozniak DJ. What's on the outside matters: the role of the extracellular polymeric substance of Gram-negative biofilms in evading host immunity and as a target for therapeutic intervention. J Biol Chem 2016;291:12538–46. https://doi.org/10.1074/jbc.R115.707547.

[17] Whitchurch CB, Tolker-Nielsen T, Ragas PC, Mattick JS. Extracellular DNA required for bacterial biofilm formation. Science 2002;295:1487. https://doi.org/10.1126/science.295.5559.1487.

[18] Koo H, Allan RN, Howlin RP, Stoodley P, Hall-Stoodley L. Targeting microbial biofilms: current and prospective therapeutic strategies. Nat Rev Microbiol 2017;15:740–55. https://doi.org/10.1038/nrmicro.2017.99.

[19] Fux CA, Shirtliff M, Stoodley P, Costerton JW. Can laboratory reference strains mirror "real-world" pathogenesis? Trends Microbiol 2005;13:58–63. https://doi.org/10.1016/j.tim.2004.11.001.

[20] Ribeiro GM, Matsumoto CK, Real F, Teixeira D, Duarte RS, Mortara RA, Leao SC, de Souza Carvalho-Wodarz C. Increased survival and proliferation of the epidemic strain *Mycobacterium abscessus* subsp. *massiliense* CRM0019 in alveolar epithelial cells. BMC Microbiol 2017;17:195. https://doi.org/10.1186/s12866-017-1102-7.

[21] Vang CK, Dawrs SN, Oberlag NM, Gilmore AE, Hasan NA, Honda JR. Comparative survival of environmental and clinical *Mycobacterium abscessus* isolates in a variety of diverse host cells. J Appl Microbiol 2022;132:3302–14. https://doi.org/10.1111/jam.15416.

[22] Kurbatfinski N, Goodman SD, Bakaletz LO. A humanized monoclonal antibody potentiates killing of diverse biofilm-forming respiratory tract pathogens by antibiotics. Antimicrob Agents Chemother 2022;66:e0187721. https://doi.org/10.1128/AAC.01877-21.

[23] Kurbatfinski N, Kramer CN, Goodman SD, Bakaletz LO. ESKAPEE pathogens newly released from biofilm residence by a targeted monoclonal are sensitized to killing by traditional antibiotics. Front Microbiol 2023;14:1202215. https://doi.org/10.3389/fmicb.2023.1202215.

[24] Mokrzan EM, Ahearn CP, Buzzo JR, Novotny LA, Zhang Y, Goodman SD, Bakaletz LO. Nontypeable *Haemophilus influenzae* newly released (NRel) from biofilms by antibody-mediated dispersal versus antibody-mediated disruption are phenotypically distinct. Biofilms 2020;2:100039. https://doi.org/10.1016/j.bioflm.2020.100039.

[25] Wilbanks KQ, Mokrzan EM, Kesler TM, Kurbatfinski N, Goodman SD, Bakaletz LO. Nontypeable *Haemophilus influenzae* released from biofilm residence by monoclonal antibody directed against a biofilm matrix component display a vulnerable phenotype. Sci Rep 2023;13:12959. https://doi.org/10.1038/s41598-023-40284-5.

[26] Goodwine J, Gil J, Doiron A, Valdes J, Solis M, Higa A, Davis S, Sauer K. Pyruvate-depleting conditions induce biofilm dispersion and enhance the efficacy of antibiotics in killing biofilms *in vitro* and *in vivo*. Sci Rep 2019;9:3763. https://doi.org/10.1038/s41598-019-40378-z.

[27] Howlin RP, Cathie K, Hall-Stoodley L, Cornelius V, Duignan C, Allan RN, Fernandez BO, Barraud N, Bruce KD, Jefferies J, Kelso M, Kjelleberg S, Rice SA, Rogers GB, Pink S, Smith C, Sukhtankar PS, Salib R, Legg J, Carroll M, Daniels T, Feelisch M, Stoodley P, Clarke SC, Connett G, Faust SN, Webb JS. Low-dose nitric oxide as targeted anti-biofilm adjunctive therapy to treat chronic *Pseudomonas aeruginosa* infection in cystic fibrosis. Mol Ther 2017;25:2104–16. https://doi.org/10.1016/j.ymthe.2017.06.021.

[28] Redman WK, Welch GS, Williams AC, Damron AJ, Northcut WO, Rumbaugh KP. Efficacy and safety of biofilm dispersal by glycoside hydrolases in wounds. Biofilms 2021;3:100061. https://doi.org/10.1016/j.bioflm.2021.100061.

[29] Zemke AC, D'Amico EJ, Snell EC, Torres AM, Kasturiarachi N, Bomberger JM. Dispersal of epithelium-associated *Pseudomonas aeruginosa* biofilms. mSphere 2020;5. https://doi.org/10.1128/mSphere.00630-20.

[30] Brockson ME, Novotny LA, Mokrzan EM, Malhotra S, Jurcisek JA, Akbar R, Devaraj A, Goodman SD, Bakaletz LO. Evaluation of the kinetics and mechanism of action of anti-integration host factor-mediated disruption of bacterial biofilms. Mol Microbiol 2014;93:1246–58. https://doi.org/10.1111/mmi.12735.

[31] Goodman SD, Obergfell KP, Jurcisek JA, Novotny LA, Downey JS, Ayala EA, Tjokro N, Li B, Justice SS, Bakaletz LO. Biofilms can be dispersed by focusing the immune system on a common family of bacterial nucleoid-associated proteins. Mucosal Immunol 2011;4:625–37. https://doi.org/10.1038/mi.2011.27.

[32] Devaraj A, Buzzo J, Rocco CJ, Bakaletz LO, Goodman SD. The DNABII family of proteins is comprised of the only nucleoid associated proteins required for nontypeable *Haemophilus influenzae* biofilm structure. MicrobiologyOpen 2018;7:e00563. https://doi.org/10.1002/mbo3.563.

[33] Swinger KK, Rice PA. IHF and HU: flexible architects of bent DNA. Curr Opin Struct Biol 2004;14:28–35. https://doi.org/10.1016/j.sbi.2003.12.003.

[34] Freire MO, Devaraj A, Young A, Navarro JB, Downey JS, Chen C, Bakaletz LO, Zadeh HH, Goodman SD. A bacterial-biofilm-induced oral osteolytic infection can be successfully treated by immuno-targeting an extracellular nucleoid-associated protein. Mol Oral Microbiol 2017;32:74–88. https://doi.org/10.1111/omi.12155.

[35] Novotny LA, Jurcisek JA, Goodman SD, Bakaletz LO. Monoclonal antibodies against DNA-binding tips of DNABII proteins disrupt biofilms *in vitro* and induce bacterial clearance *in vivo*. EBioMedicine 2016;10:33–44. https://doi.org/10.1016/j.ebiom.2016.06.022.

[36] Griffith DE. *Mycobacterium abscessus* subsp *abscessus* lung disease: 'trouble ahead, trouble behind...'. F1000Prime Rep 2014;6:107. https://doi.org/10.12703/P6-107.

[37] Engbaek H, Runyon E, Karlson A. *Mycobacterium avium* Chester: designation of the neotype strain. Int J Syst Evol Microbiol 1971;21:192–6. https://doi.org/10.1099/00207713-21-2-192.

[38] Goethe R, Laarmann K, Sproer C, Bunk B. Complete genome sequence of *Mycobacterium avium* subsp. *avium* Chester (DSM 44156). Microbiol Resour Announc 2020;9. https://doi.org/10.1128/MRA.01549-19.

[39] Johnson MM, Hill SL, Piddock LJ. Effect of carbon dioxide on testing of susceptibilities of respiratory tract pathogens to macrolide and azalide antimicrobial agents. Antimicrob Agents Chemother 1999;43:1862–5. https://doi.org/10.1128/AAC.43.8.1862.

[40] Burke A, Thomson RM, Wainwright CE, Bell SC. Nontuberculous mycobacteria in cystic fibrosis in the era of cystic fibrosis transmembrane regulator modulators. Semin Respir Crit Care Med 2023;44:287–96. https://doi.org/10.1055/s-0042-1759883.

[41] Zampoli M, Morrow BM, Paul G. Real-world disparities and ethical considerations with access to CFTR modulator drugs: Mind the gap! Front Pharmacol 2023;14. https://doi.org/10.3389/fphar.2023.1163391.

[42] Thomas D, Wessel C. The state of innovation in antibacterial therapeutics. 2022. https://www.bio.org/antibacterial-report.

[43] Novotny LA, Goodman SD, Bakaletz LO. Redirecting the immune response towards immunoprotective domains of a DNABII protein resolves experimental otitis media. NPJ Vaccines 2019;4:43. https://doi.org/10.1038/s41541-019-0137-1.

[44] Vonarburg C, Loetscher M, Spycher MO, Kropf A, Illi M, Salmon S, Roberts S, Steinfuehrer K, Campbell I, Koernig S, Bain J, Edler M, Baumann U, Miescher S, Metzger DW, Schaub A, Kasermann F, Zuercher AW. Topical application of nebulized human IgG, IgA and IgAM in the lungs of rats and non-human primates. Respir Res 2019;20:99. https://doi.org/10.1186/s12931-019-1057-3.

[45] Park IK, Olivier KN. Nontuberculous mycobacteria in cystic fibrosis and non-cystic fibrosis bronchiectasis. Semin Respir Crit Care Med 2015;36:217–24. https://doi.org/10.1055/s-0035-1546751.